Detection of Longitudinal DTI Changes in Multiple Sclerosis Patients Based on Sensitive WM Fiber Modeling

Claudio Stamile[1], Gabriel Kocevar[1], François Cotton[1,2], Françoise Durand-Dubief[1,3], Salem Hannoun[1], Carole Frindel[1], David Rousseau[1], and Dominique Sappey-Marinier[1,4]

[1]*CREATIS (CNRS UMR5220 & INSERM U1044), Université Lyon 1, INSA-Lyon, Villeurbanne, France,* [2]*Service de Radiologie, Centre Hospitalier Lyon-Sud, Hospices Civils de Lyon, Pierre-Benite, France,* [3]*Service de Neurologie A, Hôpital Neurologique, Hospices Civils de Lyon, Bron, France,* [4]*CERMEP - Imagerie du Vivant, Université de Lyon, Bron, France*

Target audience: Researchers in diffusion MRI, neuroimaging processing, neurobiologists, neurologists and MR technologists.

Purpose: White matter (WM) fiber bundles can be modeled and analyzed at any section of the bundle by merging structural information provided by tractography algorithms with metrics derived from the diffusion tensor, [1]. However, if such approach permits to detect large WM alterations, it is not sensitive enough to detect small changes affecting a limited number of fibers. Therefore, we have developed a new sensitive and automated method to detect small longitudinal variations in diffusion parameters along the fiber bundle. This method provides a local scale cross-sectional fiber bundle analysis that differentiates "pathological" fibers from "normal appearing" ones. It was applied on a weekly longitudinal follow-up of Multiple Sclerosis (MS) patients to investigate the rapid evolution of WM inflammation events.

Materials and methods: Two relapsing-remitting (RR) "untreated" MS patients' subjects were included in this study due to the occurrence of several lesions during the follow-up period. They underwent a weekly MRI exam for a period of two months that was performed on a 3T Philips Achieva System (Philips Healthcare, Best, The Netherlands). 3D FLAIR sequence was acquired to identify lesions. DTI protocol consisted in the acquisition of 60 slices of 2mm-thick using a 2D Echo Planar Imaging (EPI) sequence with 32 gradient directions (b=1000s.mm^{-2}). The analysis procedures were performed in the following order: 1) Each time point of every subject was rigidly co-registered to its first time-point. 2) Fractional anisotropy (FA) maps were generated with FSL [2]. 3) Fiber bundles were automatically extracted by a streamline probabilistic tractography algorithm [3] using as mask the JHU-Atlas ROIs [4]. 4) FA map values were associated to the fiber bundle corresponding voxels. 5) The histogram of the FA values extracted from a given bundle cross-section was fitted with a bimodal Gaussian-mixture distribution model for each time-point (Fig. 1). Significant longitudinal variations between different time-points were detected with the application of Neyman-Pearson (NP) hypothesis test on the two bimodal Gaussian-mixture models. A threshold γ given by the NP theorem was used to differentiate the bundle fibers in two subsets: fibers with FA values $\leq \gamma$ were labeled as "pathological" and fibers with FA values $> \gamma$ were labeled as "normal appearing" (Fig. 1).

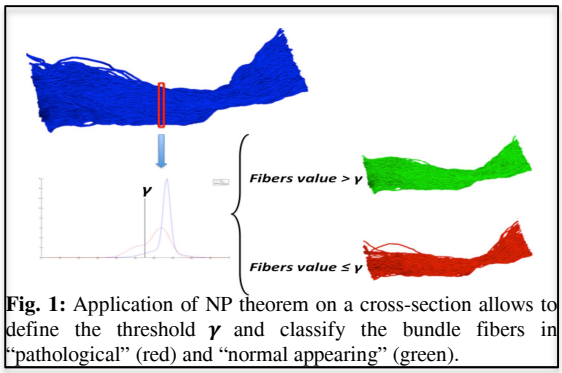

Fig. 1: Application of NP theorem on a cross-section allows to define the threshold γ and classify the bundle fibers in "pathological" (red) and "normal appearing" (green).

Results: We applied this method on two WM fiber bundles, namely the left and right Corticospinal Tracts (CST) and Inferior Fronto-Occipital Fasciculi (IFOF). As shown in Fig. 2, several longitudinal changes in FA were detected along the fiber bundle during the follow-up period. First, the presence of WM lesions corresponding to theses FA changes was confirmed on the FLAIR images. Second, the "histogram" analysis allowed to differentiate the "pathological" fibers (red) from the "normal appearing" fibers (green), which presented a similar FA profile with the first time-point (blue) used as reference (Fig. 2C-D).

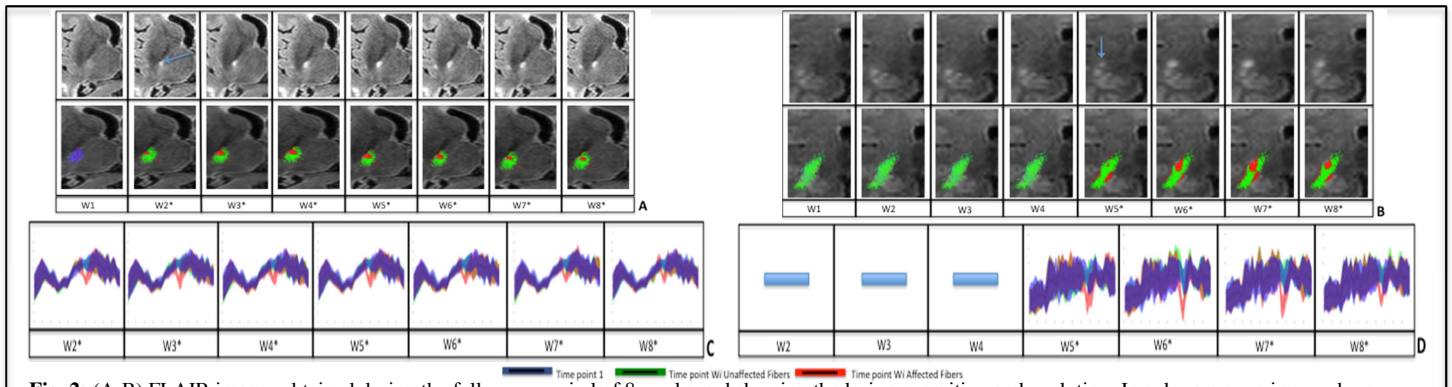

Fig. 2: (A-B) FLAIR images obtained during the follow-up period of 8 weeks and showing the lesion apparition and evolution. In color are superimposed cross-sections of fiber bundles, namely the CST (A) and the IFOF (B), divided in two fibers subsets, labeled as "pathological" (red) and "normal appearing" fibers (green). (C-D) Mean and standard deviation of FA profiles obtained along the CST (C) and IFOF (D) during 7 weeks of the follow-up period.

Discussion: We have presented a new methodology providing automatic identification of pathological fiber tracts and sensitive detection of significant longitudinal changes in diffusivity metrics. The major interest of our method consisted in its sensitivity to detect very small FA changes at multiple locations along the fiber bundle during temporal evolution. This "histogram" analysis based on the NP theorem provided two main advantages. First, the detection sensitivity was greatly improved. Second, this local scale analysis allowed to describe the WM fiber bundle in different fiber subsets, and to distinguish "pathological" from "normal appearing" fibers, both coexisting in a bundle. As confirmed by the FLAIR images, the apparition of a new lesion and its longitudinal evolution is well detected.

Conclusion: This method allowed us to characterize the microarchitecture properties of the fibers in a bundle and investigate the gradient of pathological changes along the length and the cross-section of the fiber bundle. It provides the possibility to study the longitudinal changes inside different fiber bundles and thus better understand the lesion formation in MS. This new approach offered the potential to study the relationship between lesions and distant regions of white matter as well as cortical or subcortical grey matter that are connected by a subset of "pathological" fibers. This question is of great interest since it has been previously hypothesized that WM lesions might have a role in deep grey matter atrophy in MS patients [5].

References: 1) Colby J.B., et al., Neuroimage 2012, 59:3227-3242. 2) Smith S.M., et al. Neuroimage, 2004, 23:S208-S219. 3) Tournier J., et al. Int. J. Imag. Syst. Tech. 2012, 22:53-66. 4) Hua K., et al., Neuroimage 2008, 39:336-347. 5) Henry R.G., et al., J. Neurol. Sci. 2009, 282:61-66.